JOURNAL OF MAGNETIC RESONANCE **124,** 490–494 (1997)
ARTICLE NO. MN961064

Intensity Jumping and Beating in Inversion-Recovery Experiments of Water Due to Radiation Damping

JIN-HONG CHEN, XI-AN MAO,* AND CHAO-HUI YE

Laboratory of Magnetic Resonance and Atomic Molecular Physics, Wuhan Institute of Physics, Chinese Academy of Sciences, P.O. Box 71010, Wuhan 430071, People's Republic of China

Received October 14, 1996

Nuclear spin–lattice relaxation time T_1 is an extremely important NMR parameter describing the interaction between a spin and its environment (the lattice), and is closely related to molecular dynamics. Thus, precise measurements of relaxation times are of fundamental interest. Various techniques have been developed for measuring T_1, among which the most widely used and the most reliable technique is the inversion-recovery (IR) method using the two-pulse sequence of π—τ—$\pi/2$—FID. After the π pulse, the magnetization recovers to the equilibrium state with the measured signal intensity increasing exponentially toward the equilibrium value of M_0

$$M_z = M_0[1 - 2\exp(-\tau/T_1)]. \qquad [1]$$

Generally, the constant 2 in Eq. [1] should be $1 - \cos\theta_0$ when the first pulse in the sequence is θ_0 instead of π. For samples free of radiation damping, the T_1 data obtained with IR method can be very precise. However, for concentrated samples, such as protons in solvent water, the radiation-damping effects (*1–4*) are very strong. When T_1 is negligibly small compared to the radiation-damping time T_{rd}, the recovery of the magnetization after the initial θ_0 pulse is no longer an exponential process, but is controlled by a hyperbolic tangent function (*4*):

$$M_z = M_0\tanh\{\tau/T_{rd} - \ln[\tan(\theta_0/2)]\}. \qquad [2]$$

As a result, it is impossible to measure the T_1 values by the standard IR method (*5, 6*).

Radiation damping is a physical phenomenon of concentrated samples under strong magnetic field. It results from the nonlinear coupling between the radiofrequency coil and the transverse magnetization (*1–4*). On a modern spectrometer with proton frequency higher than 500 MHz, radiation damping cannot be neglected for protons with a concentration higher than 1 mol/L (*7*). In recent years, the radiation-damping effects on T_1 measurements have been discussed in detail (*5, 6*). However, we found, in further investigations, unusual phenomena in proton IR experiments which are reported in this Communication: As the recovery time increases, the measured signal intensity decreases instead of increasing! After the arrival at the negative maximum, the intensity jumps to the positive maximum and then decreases again before finally reaching the equilibrium value. More strikingly, the intensity beats when there is a chemical-shift offset. Radiation-damping theory can give satisfactory interpretation to these interesting results.

We performed three IR experiments on proton of a water sample (90% H_2O/10% D_2O) by varying the transmitter offset with respect to the water resonance ($\Delta\omega/2\pi$ = 0, 100, 150 Hz). In order to observe the fine structure of the intensity profile, the number of the variable delay τ was as many as 110 and the value of τ was as short as 100 μs. The measured signal intensities are presented in Fig. 1 by circles and the theoretical intensities are depicted by curves. When the water signal was on resonance ($\Delta\omega$ = 0, Fig. 1A), with the increase of τ, the signal intensity went down to the negative maximum at first. Later, it suddenly jumped to the positive maximum, and then decreased gradually to a constant value (the equilibrium value). There was no increase in intensity except the sudden jump, contrasting sharply with the normal exponentially increasing curve described by Eq. [1]. When the chemical-shift offset was not zero (Figs. 1B and 1C), the sudden change from the negative maximum to the positive maximum was still observed, but in addition, there was a beat with the beat frequency in accordance with the chemical-shift offset.

The jumping and beating phenomena can only be explained by radiation-damping theory. In the usual case where radiation damping can be neglected, the signal intensity in a single-pulse experiment changes smoothly with the pulse flip angle θ_0 (following the sin θ_0 function), and the longitudinal and the transverse components of the magnetization evolve independently during the detection period according to the Bloch equations. However, in the presence of strong radiation damping, the signal-intensity profile is a sawtooth

* To whom correspondence should be addressed.

1090-7807/97 $25.00

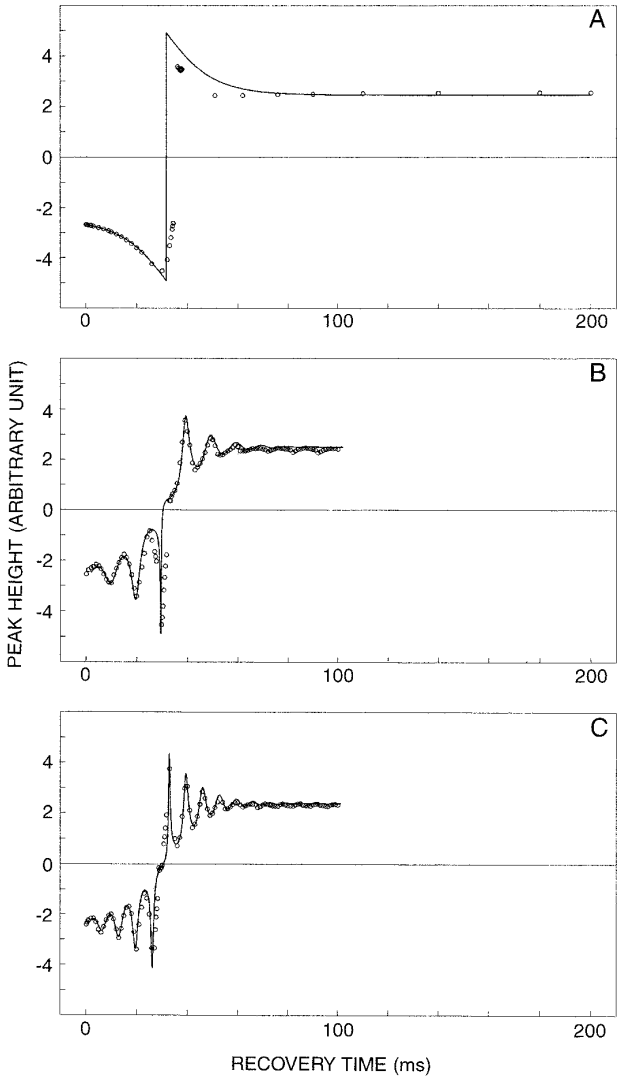

FIG. 1. The change of the water–proton-signal intensities against the recovery time in inversion-recovery experiments. The transmitter offset ($\Delta\omega/2\pi$) for (A, B, C) are 0, 100, and 150 Hz, respectively. The circles are the experimental data and the curves are the calculated results with the initial angle of $\theta_0 = 175°$ and $T_{rd} = 0.012$ s. The jumping from the negative maximum to the positive maximum can be seen in all three cases, while the beating effect can be observed only when the water signal is not on resonance.

function of θ_0 (*8*, *9*). The intensity can jump from the positive maximum to the negative maximum when θ_0 is around π. This jumping could be introduced into the IR experiments. Meanwhile, when the Bloch equations are modified by radiation damping, the longitudinal and the transverse magnetizations are coupled to each other through the T_{rd} terms even though the RF terms are missing:

$$dM_x/dt = -\Delta\omega M_y - M_x/T_2 - M_x M_z/T_{rd}M_0, \quad [3a]$$

$$dM_y/dt = \Delta\omega M_x - M_y/T_2 - M_y M_z/T_{rd}M_0, \quad [3b]$$

$$dM_z/dt = -(M_z - M_0)/T_1 + (M_x^2 + M_y^2)/T_{rd}M_0. \quad [3c]$$

Because of the coupling, the longitudinal component M_z can influence the evolution of the transverse magnetization, which have been discussed in detail (*10*). Conversely, due to the same coupling, the transverse components M_x and M_y must produce an effect on the recovery of M_z. Since the transverse magnetization oscillates (precesses) in the xy plane, the oscillation could be introduced into the longitudinal component, and in turn into the detected signal intensities in the IR experiments as a beat.

We first analyze the intensity jumping in the beat-free case with $\Delta\omega = 0$ (Fig. 1A). Compared to the radiation-damping time constant T_{rd} (=0.012 s) for the sample studied, T_1 (=2 s) and T_2^* (=0.4 s) are much longer and all the relaxation terms in Eqs. [3] can be neglected. The spin system becomes a nondecaying spin system, and the magnetization vector can be specified by a pair of angles $\theta(t)$ (the polar angle) and $\varphi(t)$ (the phase angle) with

$$\tan[\theta(t)/2] = \tan(\theta_0/2)\exp(-t/T_{rd}), \quad [4]$$

and

$$\varphi(t) = \varphi_0 + \Delta\omega t. \quad [5]$$

Equations [4] and [5] are the solutions of Eqs. [3] with relaxation neglected. The initial phase angle φ_0 is usually zero. A common view is that when a π pulse is used for inversion, θ_0 should equal π, just like $1 - \cos\theta_0 = 2$ in Eq. [1]. But for a radiation-damped sample, θ_0 cannot be replaced by π. From the mathematical point of view, $\theta_0 = \pi$ is a singular point for Eqs. [2] and [4]. Thus, although in experiments a π pulse is used, θ_0 can only be infinitively close to π. This explains why in radiation-damping-simulation studies (*9*, *11*), 179.999° and 175° have been respectively discussed but not 180°. In real situations, for a strongly radiation-damped sample, it is reasonable to let $\theta_0 = \pi - \delta$ instead of π when π pulse is involved, where $\delta \ll \pi$. This artificially introduced small angle δ accounts for the radiation-damping effect during spin inversion rather than for the inaccuracy of π in experiments (*12*), although it can indeed do for the latter purpose.

After a delay τ following the initial $\pi - \delta$ pulse, the magnetization points in a direction the polar angle of which is determined by Eq. [4] with θ_0 substituted by $\pi - \delta$ and t by τ:

$$\tan(\theta/2) = \tan[(\pi - \delta)/2]\exp(-\tau/T_{rd}). \quad [6]$$

This equation ensures θ to be always of a nonnegative value. The $\pi/2$ read pulse turns θ into

$$\theta' = \theta + \pi/2 \quad (\text{when } 0 < \theta < \pi/2) \quad [7a]$$

or

$$\theta' = \theta - 3\pi/2 \quad (\text{when } \theta > \pi/2) \quad [7b]$$

because the polar angle in the Bloch sphere is only defined in the range of $-\pi < \theta' < \pi$. The angle θ' is just the initial angle of the detected FID. According to the radiation-damping theory (*4*), the detected FID is

$$s(t) = M_0 \mathrm{sech}\{-t/T_{rd} + \ln[\tan(\theta'/2)]\}. \quad [8]$$

Consequently, in the range of the period $-\pi < \theta' < \pi$, the measured signal intensity in the frequency domain is proportional to θ' (*4, 8, 9*)

$$I = S(\omega = 0) = M_0 T_{rd} \theta' \quad (-\pi < \theta' < \pi). \quad [9]$$

Beyond this range, the intensity shows a periodical sawtooth profile.

According to Eq. [6], θ can be either greater or smaller than $\pi/2$, depending on how long the τ value is, but it cannot exceed $\pi - \delta$. Therefore, Eq. [7a] indicates a positive signal while Eq. [7b] implies a negative signal. When $\tau = 0$, $\theta = \pi - \delta > \pi/2$. From Eqs. [9] and [7b], it can be seen that $I = -M_0 T_{rd}(\pi/2 + \delta) \approx -M_0 T_{rd}\pi/2$. A negative signal is expected. With the increase of τ, θ becomes smaller and smaller (see Eq. [6]) and the absolute value of θ' becomes bigger and bigger. This explains well the initial decrease in Fig. 1A. The negative maximum of the intensity is $-M_0 T_{rd}\pi$ when θ' is infinitively close to $-\pi$ (see analysis below). Since θ is a decaying function of τ, within the remaining range of $0 < \theta < \pi/2$, which corresponds to τ being in the range of $T_{rd}\ln\{\tan[(\pi - \delta)/2]\} < \tau < \infty$, the signal intensity also decreases with the recovery time, starting from the positive maximum of $+M_0 T_{rd}\pi$. Therefore, the decrease of intensity in Fig. 1A after the jumping can also be explained. Finally when $\tau = \infty$, θ becomes zero and I will be $M_0 T_{rd}\pi/2$ (Eqs. [7a] and [9]). This is the equilibrium intensity of a radiation-damped signal in IR experiments. The signal is as strong as that of $\tau = 0$, but the phase is inverted.

The difficult case is when $\tau = T_{rd}\ln\{\tan[(\pi - \delta)/2]\}$, $\theta = \pi/2$; i.e., before the read pulse, the magnetization lies exactly on the *xy* plane. Equation [8] and consequently Eq. [9] cannot be defined in this case ($\theta' = \pi$). However, this case can indeed occur in experiments. To overcome this problem, the limiting value of θ' when θ approaches $\pi/2$ should be calculated, and this is very easy to do. When θ approaches $\pi/2$ infinitively from greater than $\pi/2$, the value of θ' must be $-\pi$. As a result, I has a negative maximum of $-M_0 T_{rd}\pi$. On the other hand, if $\theta \to \pi/2$ from less than $\pi/2$, $I = M_0 T_{rd}\pi$, the positive maximum of the intensity. So in experiments, when the magnetization recovers following the radiation-damping pathway (*5*) across the equatorial plane, i.e., when θ changes from greater than $\pi/2$ to smaller than $\pi/2$, the signal intensity jumps from $-M_0 T_{rd}\pi$ to $+M_0 T_{rd}\pi$. The theoretical intensities calculated with $\delta = 5°$ and $T_{rd} = 12$ ms based on the analysis above are shown as a curve in Fig. 1A, in agreement with the experimental results (the circles). The discrepancies around the ''jumping'' may be due to the disturbance from the transmitter. Because the signal is ''on resonance,'' the transmitter can on one hand cause a small phase problem and on the other hand bring about a small artifact, called a transmitter artifact, both affecting the signal intensity measurement.

An intuitive picture is depicted in Fig. 2 shown with the *yz* cross section of the Bloch sphere. Just before the read pulse, the magnetization can be either in the south (B, Route I) or in the north (B, Route II). When in the south, it will be driven onto the west side by the read pulse (C, Route I), and a clockwise rotation due to radiation damping toward equilibrium will occur (D, Route I). This leads to a negative signal. Otherwise, the magnetization rotates anticlockwise, resulting in a positive signal (Route II). The shaded areas in D are proportional to the corresponding areas of the FID which are just equal to the intensities in the frequency domain according to the area theorem of the Fourier transformation (*13*). The intensity jumping from negative to positive can be understood by the continuous change of the magnetization vector from the east to the west through the south pole in C. If the spin system is free of radiation damping, the continuous change of θ' from $\pi - \delta$ to $\pi + \delta$ brings about continuous change in intensity following a sine function. Although there is a sign change when θ' is around π, the intensity jumping can never be expected.

When there is a transmitter offset, precession of the transverse magnetization during the recovery must be taken into account. It is easy to analyze the evolution of the spin-density operator $\sigma(\tau)$. For the radiation-damped spin system, during the recovery τ period,

$$\sigma(\tau) = I_x \sin\theta(\tau)\sin\varphi(\tau) + I_y \sin\theta(\tau)\cos\varphi(\tau) + I_z \cos\theta(\tau) \quad [10]$$

with $\theta(\tau)$ and $\varphi(\tau)$ determined according to Eqs. [4] and [5], respectively. The following $\pi/2$ (assumed in the *x* direction) read pulse changes Eq. [10] into

$$\sigma(\tau_+) = I_x \sin\theta(\tau)\sin\varphi(\tau) - I_z \sin\theta(\tau)\cos\varphi(\tau) + I_y \cos\theta(\tau), \quad [11]$$

where τ_+ denotes the instant just behind the $\pi/2$ pulse. If at this moment the direction of the magnetization is described by a new pair of angles $\theta'(\tau_+)$, $\varphi'(\tau_+)$, we must have

$$M_x = M_0 \sin\theta'(\tau_+)\sin\varphi'(\tau_+), \quad [12a]$$

$$M_y = M_0 \sin\theta'(\tau_+)\cos\varphi'(\tau_+), \quad [12b]$$

$$M_z = M_0 \cos\theta'(\tau_+). \quad [12c]$$

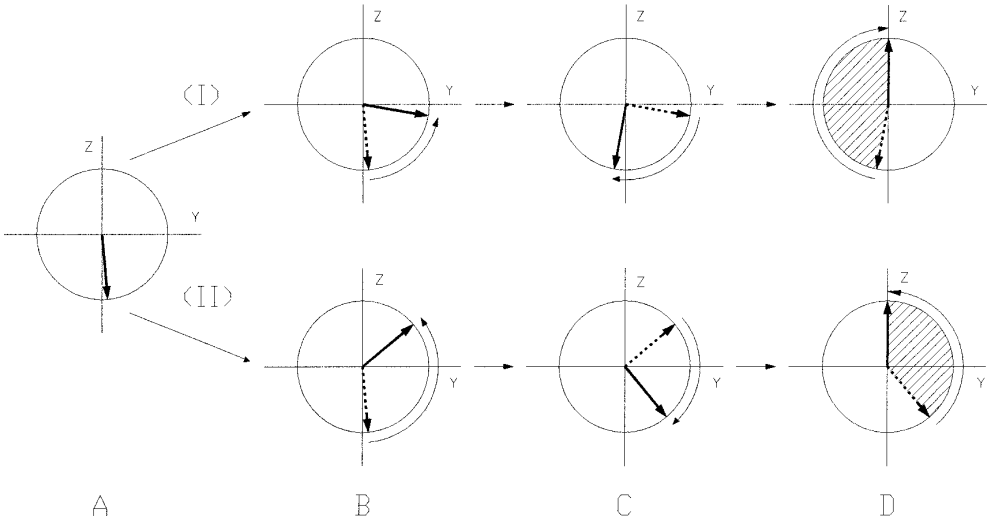

FIG. 2. Diagram for inversion recovery of the strongly radiation-damped magnetization. Transmitter offset is zero so only the *yz* cross section of the Bloch sphere is shown. Either under the RF pulse or under radiation damping, the trajectory of the magnetization vector is on the surface of the sphere. (A) The initial state of the magnetization before recovery. (B) Recovery due to radiation damping. (C) Rotation by the read $\pi/2$ pulse. (D) During the detection period. In (A), the magnetization is inverted by a π—δ pulse where the small angle δ accounts for the radiation-damping effect during spin inversion. Following Route I, a negative signal is expected, but following Route II one has a positive signal. If τ is shorter than $T_{rd}\ln\{\tan[(\pi - \delta)/2]\}$, just before the read pulse, the magnetization is in the southern part (IB); otherwise, it is in the northern part (IIB). After the read $\pi/2$ pulse, the magnetization can be either in the western (IC) or in the eastern part (IIC), depending on how long the recovery time is. The west magnetization leads to a negative signal with the intensity corresponding to the shaded area, while the east magnetization results in a positive signal. When the magnetization moves from the west to the east through the south pole, there is an intensity jump from the negative maximum to the positive maximum.

By comparing Eqs. [12] with Eq. [11], we can readily write

$$\theta'(\tau_+) = \cos^{-1}[-\sin\theta(\tau)\cos\varphi(\tau)], \quad [13a]$$

$$\tan\varphi'(\tau_+) = \tan\theta(\tau)\sin\varphi(\tau). \quad [13b]$$

In the subsequent detection period, the magnetization evolves according to

$$s(t) = M_0\,\mathrm{sech}\{-t/T_{rd} + \ln[\tan(\theta'/2)]\} \times \exp[i(\Delta\omega t + \varphi')]. \quad [14]$$

The FID described by Eq. [14] yields the signal intensity in the frequency domain

$$I = S(\omega = \Delta\omega) = M_0 T_{rd}\theta'(\tau_+)\cos[\varphi'(\tau_+)]. \quad [15]$$

It is apparent that the intensity is a complicated triangular function of $\Delta\omega\tau$, and a beating effect is expected. The curves in Figs. 1B and 1C are the numerically calculated results based on Eq. [15]. Very good agreement with the experimental data (the circles) has been achieved.

Equation [15] is the general intensity formula for a strongly radiation-damped signal in inversion-recovery experiments. If $\Delta\omega = 0$, according to Eq. [5] $\varphi(\tau) = 0$. Hence, $\varphi'(\tau) = 0$ (see Eq. [13b]). There is no longer any oscillation. In this case, Eq. [15] is reduced to Eq. [9] and the beating effect vanishes.

This study shows once again that the IR technique cannot be used for measuring the spin–lattice relaxation time of a radiation-damped sample. If someone happens to use this technique, and in his experiments, the interval of τ is bigger than the reciprocal of the chemical-shift offset ($\tau > 1/\Delta\omega$), neither jumping effect nor beating effect in the intensity could be observed. If in this case data fitting to the exponential equation [1] is forced, a great error in T_1 will result, which will prevent making a valid dynamic conclusion.

In summary, the jumping and beating effects of the signal intensity in inversion-recovery experiments for radiation-damped samples have been demonstrated for the first time and quantitatively analyzed. Two points as far as radiation damping is concerned are of great importance and should be emphasized. The first one is that under strong radiation damping, the magnetization remains coherent (undephased), as can be described at any time by a set of equations like Eqs. [12]. Hence, the initial polar and phase angles of the detected FID are modulated by both radiation damping and precession during the recovery period, much like the radiation-damped FID in 2D experiments (*14, 15*). The second point is that the polar angle π should be avoided in radiation-damping analysis, even if the π pulse in experiments is accurate. This has been used for analyzing radiation-damping-induced half-frequency-spaced artifacts in 2D *J*-resolved spectra (*12*).

ACKNOWLEDGMENT

This work was supported by the National Natural Science Foundation of China.

REFERENCES

1. A. Abragam, ''The Principles of Nuclear Magnetism,'' Clarendon, Oxford, 1961.
2. N. Bloembergen and R. V. Pound, *Phys. Rev.* **95,** 8 (1954).
3. W. S. Warren, S. L. Hames, and J. L. Bates, *J. Chem. Phys.* **91,** 5895 (1989).
4. X.-A. Mao and C.-H. Ye, *J. Chem. Phys.* **99,** 7455 (1993).
5. X.-A. Mao, J.-X. Guo, and C.-H. Ye, *Chem. Phys. Lett.* **222,** 417 (1994).
6. D. Wu and C. Johnson Jr., *J. Magn. Reson. A* **110,** 113 (1994).
7. X.-A. Mao, J.-X. Guo, and C.-H. Ye, *Chem. Phys. Lett.* **218,** 249 (1994).
8. X.-A. Mao, D. Wu, and C.-H. Ye, *Chem. Phys. Lett.* **204,** 123 (1993).
9. J. Virlet, *J. Chim. Phys. Phys. Chim. Biol.* **89,** 515 (1992).
10. J.-X. Guo and X.-A. Mao, *Phys. Rev. B* **50,** 13461 (1994).
11. A. Vlassenbroek, J. Jeener, and P. Broekaert, *J. Chem. Phys.* **103,** 5886 (1995).
12. J.-X. Guo and X.-A. Mao, *J. Phys. II France* **6,** 1183 (1996).
13. D. C. Champeney, ''Fourier Transforms and Their Physical Applications,'' Chap. 2, Academic Press, London, 1973.
14. X.-A. Mao, J.-X. Guo, and J.-H. Chen, *J. Phys. D* **29,** 1595 (1996).
15. J.-H. Chen, X.-A. Mao, and C.-H. Ye, *J. Magn. Reson. A* **123,** 126 (1996).